8-2014

3-D Morphometric Analysis of the Primate Elbow Joint

Seth Brockman Boren
University of Arkansas, Fayetteville

3-D Morphometric Analysis of the Primate Elbow Joint

3-D Morphometric Analysis of the Primate Elbow Joint

A thesis submitted in partial fulfillment
of the requirements for the degree of
Master of Arts in Anthropology

By

Seth Boren
Hendrix College
Bachelor of Arts in Biology and Sociology and Anthropology, 2012

August 2014
University of Arkansas

This thesis is approved for recommendation to the Graduate Council.

_____
Dr. J. Michael Plavcan
Thesis Director

_____
Dr. Peter S. Ungar
Committee Member

_____
Dr. Justin M. Nolan
Committee Member

Abstract

Large body size requires limb joints capable of supporting said weight, and a species exhibiting sexual size dimorphism may necessitate joint size differences between the sexes of the species. If habitual behavior differs with body size, one may expect to see significant variation in joint morphology between species and the sexes within species. The following analysis tests two hypotheses: (1) that significant differences in joint size between males and females correlate with the magnitude of sexual dimorphism and (2) that there is significant interspecific variance in joint shape between males and females of the same species. The first hypothesis is tested by taking principal component scores from the first two components of a Principal Component Analysis (PCA) with full tangent space and Procrustes form space projection and subjecting them to an Analysis of Variance (ANOVA) to see if a significant amount of variance exists between sexes for each species observed. The second hypothesis is tested in the same way, the only difference being that the PCA utilizes solely a full tangent space projection in order to nullify size differences in variance. The results of the analysis show that the magnitude of sexual dimorphism correlates with differences in joint size. However, there is no significant interspecific variation in shape between males and females in the same species. The analysis did not have a consistent sample size for all sexes or species and the sample sizes were all relatively small. As such, an analysis with larger samples and greater consistency will be needed to confirm the inferred conclusions.

Table of Contents

I.) Introduction

The primate elbow joint is adapted to bear weight in tension and compression and to provide stability during flexion and extension (Feldesman, 1976; Feldesman 1982; Rose 1988; Ruff and Runestad 1992; Rockwell 1994; Lague and Jungers 1999; Lague 2003; Drapeau 2008). At the same time, there is significant variation in the locomotor and postural behavior, body size, and body size dimorphism throughout primates (Feldesman 1976; Doran 1993 (1); Doran 1993 (2); Plavcan 2001; Patel 2005 (2); Drapeau 2008), all of which can have a substantial impact on the types of loads transmitted through the elbow. Large body size necessitates limb joints capable of supporting large weights, and differences in weight associated with sexual size dimorphism may necessitate differences in limb joint morphology between the sexes (Lague 2003). If body size and habitual behavior vary significantly within and between primate species, we should likewise expect to see significant variation in elbow joint morphology within and between species. My analysis will evaluate size and shape variation of the articulation of the proximal ulna among a series of anthropoid primates and examine the ways that shape variation corresponds to variation in habitual locomotor behavior, body size, and body size dimorphism.

The following study will test two hypotheses: (1) that significant differences in joint size between males and females correlate with the magnitude of sexual dimorphism, (2) that there is significant interspecific variation in joint shape between males and females (in a given species).

A.) Anatomy of the Proximal Ulna

As a group, modern primates share the primitive therian mammalian forelimb morphology, with the radius and ulna unfused. The elbow is comprised of three joints: the humeroulnar, humeroradial, and radioulnar. The humeroulnar joint comprises the articulation of the trochlear surface of the proximal ulna against the trochlear surface of the distal humerus. The humeroulnar joint, being a classic saddle joint, allows only for flexion and extension. The humeroradial joint, in contrast, accommodates both flexion and extension and the rotation of the radius in association with supination and pronation of the forearm. This is accomplished by the articulation of the rounded, cup-like surface of the proximal radius against the toroid surface of the humeral capitulum. This configuration allows rotation of the proximal radial head against the humerus through a continuous range of flexion and extension. Finally, contact between the proximal radial head and the proximal ulna results in the radioulnar joint, which accommodates rotation of the radial head against the ulna. Notably, weight is born primarily through the humeroulnar joint (Feldesman 1976; Rockwell 1994; White et al. 2012).

Motions about the elbow are controlled by a series of flexors and extensors, a series of muscles that control supinators and pronators, and secondarily by the attachment of the flexors and extensors of the wrist and hand, which cross the elbow and attach to the humerus. Amongst all primates, flexion is facilitated by the insertion of the *biceps brachii* on the radial tuberosity while extension is facilitated by the insertion of the *triceps brachii* on the olecranon of the elbow (Diego et al. 2012; White et al. 2012). The *pronator teres muscle* inserts on the lateral radial shaft to accommodate pronation and the *supinator muscle* inserts on the radial tuberosity to provide supination. The *biceps brachii* also provides for supination whilst the forearm is pronated (White et al. 2012).

The elbow is stabilized by a series of ligaments that allow for movement while resisting dislocation. The ligaments in the elbow are partitioned into two collateral ligament complexes; the medial and the lateral. In the lateral collateral ligament complex, the positions of the radius and the ulna relative to the humerus are maintained by the radial and ulnar collateral ligaments, which both originate from the lateral epicondyle. The radial collateral ligament inserts on the annular ligament and the ulnar collateral ligament inserts on the lateral side of the ulna. The annular ligament extends from the ulna and wraps around the head of the radius, holding the bones of the forearm together. The medial collateral ligament complex is made up of anterior and posterior bundles, both of which originate on the medial epicondyle of the humerus and insert on the medial coronoid process. The oblique chord ligament originates from the coronoid process on the anterolateral aspect of the ulna and inserts just below the radial tuberosity on the posteromedial aspect of the radius, stabilizing the elbow during quadrupedal locomotion. The oblique cord is present in all Old World monkeys, but is variable in *H. sapiens* and *P. troglodytes* (Regan et al. 1991, Patel 2005 (1), Diego and Wood 2011, Diego et al. 2012, White et al. 2012).

No muscles in the modern human elbow are unique to humans; the general musculature of the elbow joint is plesiomorphic throughout primates, though there are derived features in some taxa. Synapomorphic among most hominoids, with the exception of *Pan*, is the loss of the *epitrochleoanconeus,* a muscle ancestral to tetrapods that connects the medial epicondyle of the humerus to the olecranon process of the ulna. Amongst modern humans, *Hylobates*, *Pongo*, and *Gorilla* the *epitrochleoanconeus* is not present as a separate, well-defined muscle with the exception of rare cases (Abdala and Deigo 2010, Diego et al. 2012). Amongst hylobatids the *pronator teres* typically originates solely from the humerus, reflecting the ancestral state. In

hominids, however, the *pronator teres* is slightly derived, usually originating from both the humerus and ulna (Diego and Wood 2011, Diego et al. 2012; White et al. 2012).

B.) Shape and Size Differences and Dimorphism

Richmond (1998), given the correlation between function and joint morphology, shows that it is possible to distinguish between hominoids, cercopithecoids and platyrrhines based on the morphology of the ulna.

The differences in the specific shape and size of a given articular surface correlate with the magnitude of transmitted forces, the position of the joint during loading, and the range of motion necessary during locomotion (Ruff and Runestad 1992). There are two trends in catarrhine morphology: one trend for forearm rotational mobility, exhibited by hominoids, and another for terrestriality, exhibited by cercopithecoids (Richmond et al. 1998; Schmitt 2003).

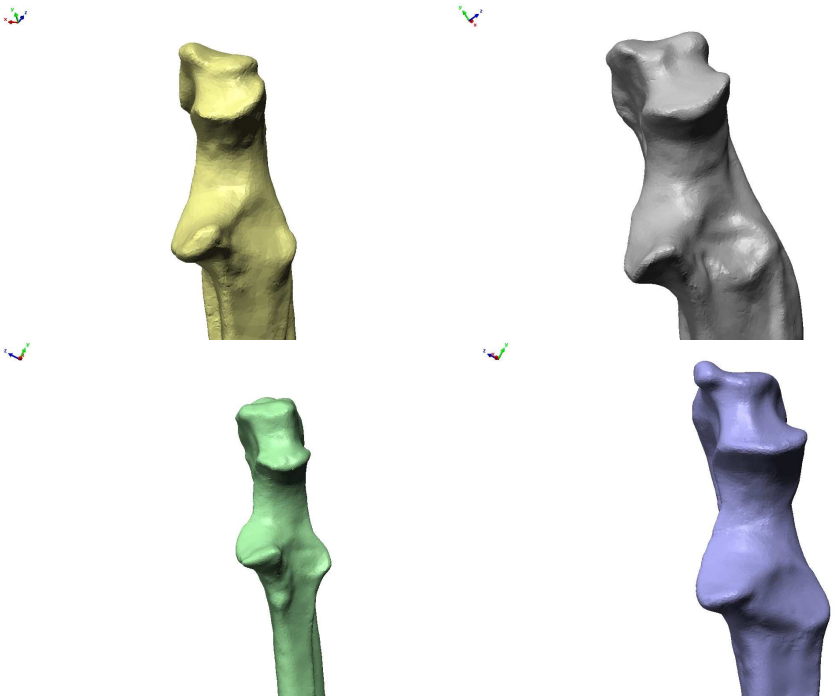

Figure 1.) Cercopithecoid and basal catarrhine ulnas. From left to right, top to bottom: female *Macaca nemestrina,* male *Cercocebus torquatus,* male *Cercopithecus alboguris kolbi,* male *Colobus guereza kikuyuensis*.

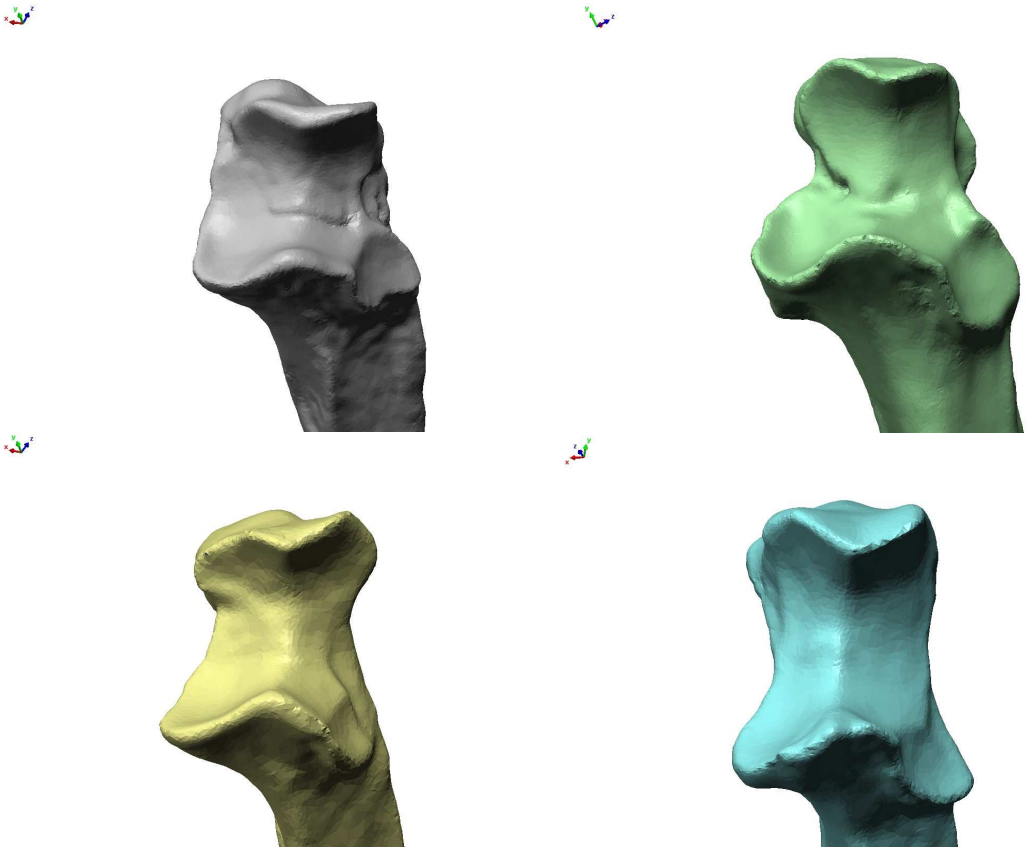

Figure 2.) Hominoid ulnas. From left to right, top to bottom: Male *Gorilla gorilla*, male *Pongo pygmaeus*, male *Pan paniscus*, male *Pan troglodytes*.

The primitive form of the anthropoid ulna is exhibited by platyrrhines and basal catarrhines (Figure 1), wherein the radial head is positioned anteriolaterally to the proximal ulna and anteriorly overlaps with one half the width of the ulnar shaft. Cercopithecoids typically exhibit a narrow trochlear surface, deep and narrow sigmoid notches and olecranon processes, and a wide, anteriorly facing radial notch. Hominoids, likewise, exhibit relatively broad and low trochlear notches with marked median ridges, reduced olecranon processes, laterally facing radial notches, and prominent lateral trochlear rim, which provides elbow stability in all phases of flexion and extension (Jenkins 1973) (Figure 2). Cercopithecoids exhibit a limited, laterally facing area of the trochlear notch for articulation with the lateral side of the humeral trochlea; hominoids exhibit an articulation with the medial trochlear keel occupying the whole length of

the trochlear notch (Jenkins 1973; Feldesman 1976; Rose 1988; Richmond et al. 1998). The forelimb is subjected to either tensile stress or to muscle generated compressive stresses. During suspensory locomotion the forelimb experiences predominately tensile loading and reduced compressive loading (Swartz 1989). Hominoids frequently use suspensory locomotion to navigate arboreal environments, placing the elbow joint in tension. The pronounced hominoid trochlear keel inhibits the radial head from overriding the capitulum during suspensory behavior (Rockwell 1994). Terrestrial quadrupedal primates (such as baboons and great apes, hylobatids being solely suspensory) possess elbow joints better prepared to resist mediolateral forces, specifically those that would cause medial collapse at the elbow. Terrestrial primates regularly experience lateral and medial oriented substrate reaction forces, which may explain the robust keeling exhibited on both sides of the humeral articular surface of the elbow (Schmitt 2003).

Body size and locomotor behavior are the primary factors that dictate the nature of skeletal stresses and thereby strongly influence the morphology of skeletal elements. Joints support the body of an organism, and as body size increases joint shape can change to better support weight (Swartz 1989; Lague 2000; Lague 2003). As such, the effect of body size on joints has been shown to be pivotal in interpreting skeletal structure variation in a functional context (Gould 1966, Ruff and Runestad 1992). The linear dimensions of bones will vary in proportion to body mass at a power of 1:3 if there is no variation in shape associated with body size variation. If shape remains constant as size changes in a given bone, the surface or cross-sectional areas of the bone (proportional to the square of the linear dimensions) will vary in proportion to body mass at a power of 2:3. If peak forces exerted on a limb are directly related to the force exerted due to gravity acting on body mass, then the loads which the limb bears will also increase in proportion to body mass. With isometric scaling, peak stress will be greater in

the bones of larger animals (Gould 1966, Swartz 1989). Thus, as body size varies between vertebrate species, one can expect to see different sizes of joints in the skeletons of said species. Dimorphism can be viewed as an extension of the relationship between body size and joint form. Just as species with differing body weights can be expected to have different joint sizes, males and females of a single species can be expected to have different joint shapes if a significant degree of size dimorphism is present in the species (Plavcan 2001).

Sexual size dimorphism is prevalent amongst anthropoid primates. Weight bearing is a major constraint on the design of joints (Swartz 1989). Males are on average larger than females among anthropoid species (Plavcan 2011). Amongst anthropoid species, extant catarrhines are known to exhibit a relatively high degree of body size dimorphism (Fairbairn 1997, Plavcan and Schaik 1997). Amongst *Pongo abelii*, for example, males on average weigh twice as much as females (Cant 1987). Male cercopithecoids exhibit body masses ranging from 30-80% larger than female cercopithecoids. Dimorphism in the elbow joint articulation can be present in two respects: size and shape. Differences in joint size and shape are not mutually exclusive; a joint can exhibit a high degree of shape dimorphism yet have little to no size dimorphism, and vice versa (Lague 2000). For a given size dimorphic primate species, males are expected to have larger limb joints than one would expect based on isometric scaling of joint size to body size (Gould 1966, Plavcan and Schaik 1997; Plavcan 2001; Lague 2000).

Skeletal dimorphism typically arises as a consequence of size dimorphism and not as a consequence of varying selection for different male and female adaptations (Fairbairn 1997, Plavcan 2001). However, size dimorphism can lead to differences in locomotor behavior. Large primates, by virtue of their size, cannot support their bodyweight by moving quadrupedally along arboreal substrates (Cant 1987, Schmitt 2003). As body size increases, one can expect to

observe a decrease in the frequency of leaping behavior and an increase in the frequency of suspensory behavior (Rockwell 1994). Cant observed that male *P. abelii*, due to their greater bodyweight, more frequently utilize above-branch postures while feeding than females. In comparison, female *P. abelii* more often utilize below-branch postures while feeding. The males also typically feed on larger substrate branches than females in order to support their weight during feeding, females being light enough to hang from smaller branches (Cant 1987). Doran has shown that even closely related species, such as *Pan troglodytes* and *Pan paniscus*, can exhibit differences in morphology and locomotion based on body weight. In comparison to *P. troglodytes*, *P. paniscus* utilize more quadrupedalism and less quadrumanous climbing and scrambling. *P. paniscus* are typically smaller in size than chimpanzees, thus they are able to more frequently find arboreal substrates capable of supporting their weight when practicing arboreal quadrupedalism. *P. paniscus* females also more frequently utilize arboreal quadrapedalism than their larger male counterparts, showing how locomotor behavior can differ between sexes. *P. paniscus* arboreal quadrupedalism is primarily palmigrade, which is unusual given how important suspensory behavior is in the locomotor repertoire of great apes. *P. troglodytes* almost always knuckle-walk during arboreal quadrupedalism; this is so they can retain their adaptations for hanging, a vital component for scrambling and climbing behavior (Doran 1993(1); Doran 1993(2)).

The biomechanical and functional reasons for variation in patterns of dimorphism are not well understood and little comparative work has been done on the subject (Plavcan 2001). There are few analyses of sexual dimorphism in the limb joints, and most studies of sexual dimorphism in the elbow joint have focused on the humerus (Jenkins 1973; Lague and Jungers 1999; Lague 2000). The likelihood of significant dimorphism in relative size for a joint surface should be

related to the degree of body size dimorphism and the magnitude of peak stresses that are habitually encountered by the joint. Large males can encounter relatively greater joint stress levels than females unless structural change compensates for increased weight-related forces (Lague 2000). Lague's study of joint size dimorphism found that cercopithecine monkeys tend to have relatively large degrees of joint size dimorphism in the distal humeral joint articulation. Nonhuman hominoids were found to typically exhibit low joint size dimorphism; even species with high body weight dimorphism, such as *P. pygmaues* and *Gorilla gorilla*, were found to have geometrically similar joint sizes between sexes. Modern humans, despite not using their elbow joints to support bodyweight, were found to exhibit a relatively higher degree of joint size dimorphism than other hominoids (Lague 2003). Lague and Jungers found that catarrhines do not exhibit sex-related shape differences in the distal humerus, the only exception being *G. gorilla*, which exhibited a more expanded trochlear crest in males than in females (1999).

Joint scaling patterns have pivotal implications for the analysis of sexual dimorphism. To maintain joint stresses, large animals may exhibit disproportionately larger joint surfaces than smaller animals, resulting in shape differences that significantly deviate from isometric scaling (allometry). Positive allometry indicates morphology that increases in size faster than body size increases. Negative allometry, likewise, indicates morphology that increases in size slower than body size increases. Isometry is when morphology increases in size at a rate proportional to body size, so that geometric proportionality is maintained at all sizes (Rockwell 1994). Swartz identified positive interspecific allometry, with the larger joints of larger primates exhibiting significant intraspecific scaling (1989). Godfrey found that the joint articulations of primates, particularly in the humerus, exhibit positive allometry (1991). Ruff and Runestad note that anthropoid primates exhibit isometric or at least modest positive allometric scaling in the

morphology of diaphyseal cross sections. Primates appear to follow the same general scaling trends in their limbs as other mammals. However, specific size-related modifications may have different effects on different structural properties (Ruff and Runestad 1992). Joint surface allometry in entirely suspensory primates, such as gibbons, is found to not significantly deviate from the overall anthropoid pattern. In the case of gibbons, locomotor repertoires that reduce limb loading may have no selective effect on joint morphology. Gibbon morphology may in fact reflect the biomechanics of the ancestral locomotor condition (Swartz 1989).

Little research has been done in regards to how sexual dimorphism can influence joint articulator size and shape. My analysis will investigate how joint size and shape change with body size in primates. Morphometrics and multivariate analyses will be used to examine how variance in joint size and shape are distributed in *Hylobates lars*, *Pongo pygmaeus*, *Papio cynacephalous*, *Gorilla gorilla*, *Pan paniscus*, *Pan troglodytes*, and *Homo sapiens*, specifically testing the hypothesis that joint shape and size vary significantly between males and females in each species. The analysis will examine how variance is distributed across eigenvectors from two separate Principal Component Analyses: one with Procrustes Form Space Projection and one without. Principal component scores from each eigenvector will be used in several Analyses of Variance to examine whether or not shape and size vary significantly between males and females in each species. If species and sexes exhibit a significant difference in a given set of principal component scores, then one can conclude that variations exists in the morphology of joint articulation of the proximal ulna.

II.) Methods

The comparative sample for the analysis consists of 10 *Hylobates lars* (4 male, 6 female), 13 *Pongo pygmaeus* (6 male, 7 female), 21 *Papio cynacephalus* (11 male, 10 females), 14 *Gorilla gorilla* (7 male, 7 female), 16 *Pan paniscus* (8 males, 8 females), 20 *Pan troglodytes* (9 males, 11 females), and 35 *Homo sapiens* (16 male, 19 female) ulnas. All individuals are adult as judged by epipheseal fusion. The sample is meant to be representative of the Hominoidea, with *P. cynacephalus* as an out-group and a representative of Cercopithecoidea. The primates analyzed practice a wide variety of locomotor behavior. *P. cynacephalus* are terrestrial quadrupeds, *H. lars* are brachiators, and *H. sapiens* are bipeds. With the exception of *H. sapiens*, the great apes analyzed practice a mosaic of arboreal and terrestrial locomotor behavior; preferences for any one locomotor behavior vary depending on the environment of a given population. *P. pygmaeus* practices a combination of suspension and clambering in arboreal environments while terrestrially being a fist-walker. *P. troglodytes*, *P. paniscus*, and *G. gorilla* are all terrestrial knucklers and arboreally practice a combination of suspension and clamber. All of the ulnas were taken from the 3-D model collection collected by Dr. J. Michael Plavcan at the University of Arkansas. The models were scanned using a Konica-Minolta Vivid 9i 3-D scanner and then uploaded and rendered in Polyworks software. All the ulnas were either from the left side, or were right ulnas mirrored to match a left ulna. The 3-D coordinates of articular landmark sites were collected using Polywork's IMinspect. Twenty-two landmarks were taken off of the humeroulnar and radioulnar articulators to record the shape of the ulna proximal joint articulations. The landmarks on the humeroulnar and radioulnar articulators were chosen based on the location of landmarks identified by Feldesman and Drapeau, with midpoints chosen to more accurately map joint shape (1976, 2008). The landmarks are tips, extrusions, extremal

points, and mid-points between other landmarks along the edge of the joint articulation (Figure 3, Table 1).

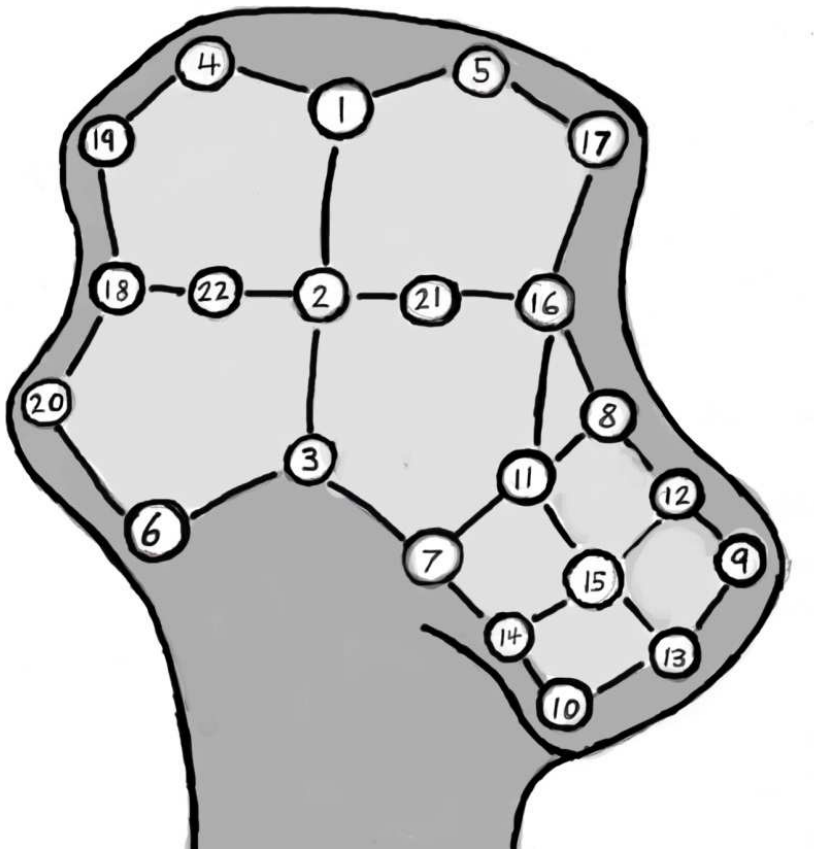

Figure 3.) Ulna Landmarks. Each circle represents a landmark. The numbers inside each circle correspond to the landmarks in Table 1.

Table 1.) Ulna Landmarks

Ulna Landmarks			
#	Landmark	#	Landmark
1	Anconeal Beak	13	Midpoint between 9 and 10 (Distal border of RA)
2	Keel Midpoint	14	Midpoint between 7 and 10 (Anterior border of RA)
3	Coronoid Process	15	Midpoint between 11 and 13 (Center of RA)
4	Anteromedial Border of HA	16	Midpoint between 5 and 7 (Lateral Facet of HA)
5	Anterolateral Border of HA	17	Midpoint between 5 and 16 (Proximal Lateral Facet of HA)
6	Posteromedial Border of HA	18	Midpoint between 4 and 6 (Medial Facet of HA)
7	Proximal Anterior Border of RA	19	Midpoint between 4 and 18 (Proximal Medial Facet of HA)
8	Proximal Posterior Border of RA	20	Midpoint between 6 and 18 (Distal Medial Facet of HA)
9	Distal Posterior Border of RA	21	Midpoint between 2 and 16 (Center of Lateral HA)
10	Distal Anterior Border of RA	22	Midpoint between 2 and 18 (Center of Medial HA)
11	Midpoint between 7 and 8 (Proximal border of RA)	Key: HA - Humeroulnar Articulaton, RA - Radioulnar Articulation	
12	Midpoint between 8 and 9 (Posterior border of RA)		

To place midpoint landmarks along the rim of the humeroulnar articulation, a plane (Plane A) is anchored to the two landmarks (Points A and B) being intersected by the midpoint landmark and a floating point (Point C) placed at the midpoint between the anconeal beak and coronoid process. In Figure 4, point A is the anteromedial most point on the border of the humeroulnar articulation (Landmark 4), while point B is the postermedial most point (Landmark 6). Once plane A is identified, a line (Line A) passing through points A and B is plotted along plane A and the midpoint between points A and B is identified (Point D). A line (Line B) perpendicular to line A is plotted on plane A through point D. Finally, the midpoint landmark

(Landmark 18) is plotted on the rim of the joint articulation at a point along a line perpendicular to plane A that intersects line B. The midpoint along the rim of the humeroulnar is identified as the midpoint between points A and B for the analysis. Midpoints on the humeroulnar articulator (Landmarks 16-20) were placed using the described method (Figure 4).

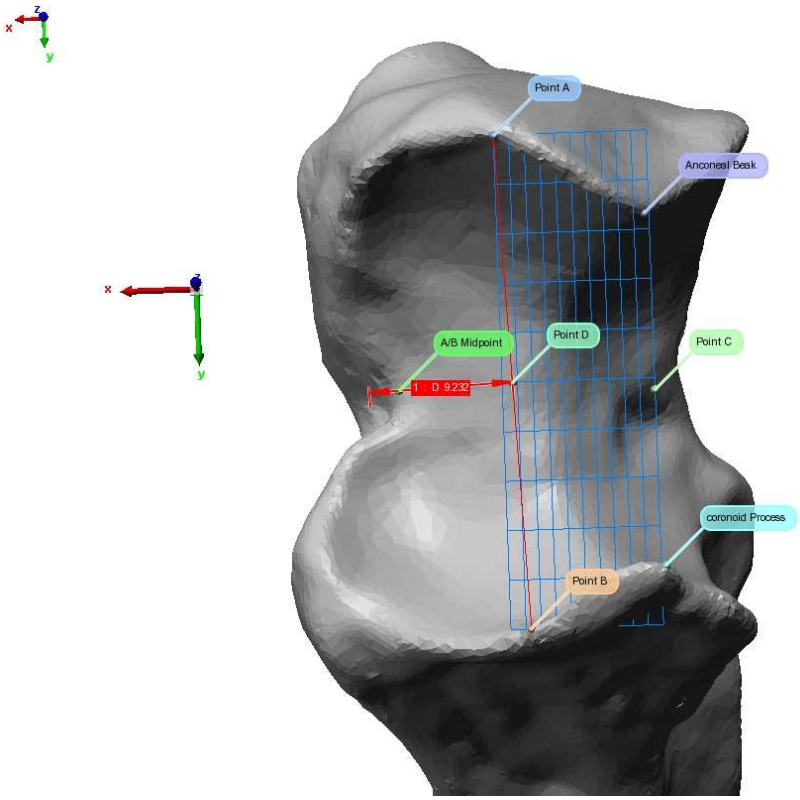

Figure 4.) Male *Homo sapien* ulna (Hosap 496). Points, planes, and lines for placing midpoint landmarks on the humeroulnar articulation. The midpoint landmark is along a line perpendicular to Plane A. Line A is shown in red. Plane A is shown in blue.

To identify the keel midpoint (Landmark 2), a plane (Plane B) is anchored to the anconeal beak, coronoid process, and the ulnar keel. A line (Line T) is plotted through the landmarks on the anconeal beak and coronoid process. The midpoint between the anconeal beak and the coronoid process along line T on plane B is identified (Point C). A line (Line C) perpendicular to line T is plotted through point C on plane B. The point where line C intersects the ulnar keel is identified as the keel midpoint (Figure 5).

The center of the lateral humeroulnar (Landmark 21) is placed by finding the midpoint between the keel midpoint (Landmark 2) and the lateral facet of the humeroulnar (Landmark 16). The midpoint between keel midpoint and lateral facet of the humeroulnar along the surface of the joint is chosen as center of the lateral humeroulnar. This same method is use to place the center of the medial humeroulnar (Landmark 22) which is the midpoint between the keel midpoint and the medial facet of the humeroulnar (Landmark 18).

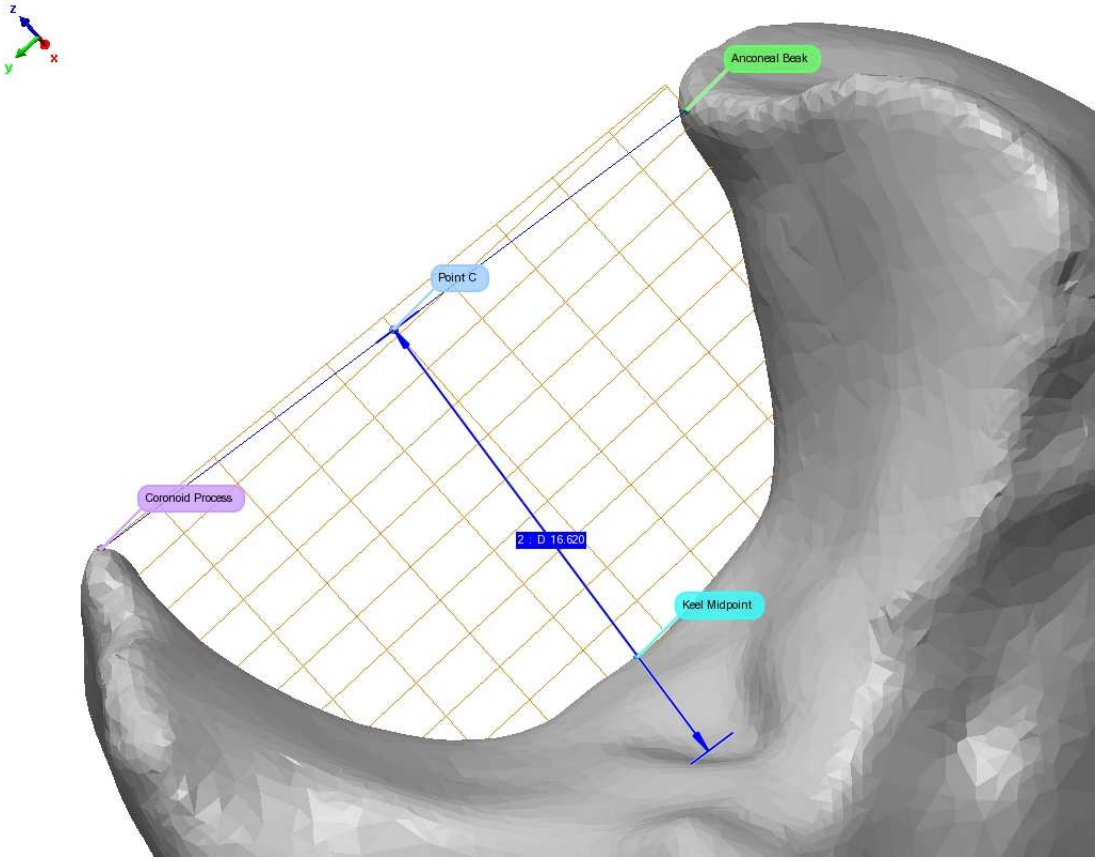

Figure 5.) Male *Homo sapien* ulna (Hosap 496). Points, planes, and lines for placing the Keel Midpoint. Line C is shown in blue. Plane B is shown in orange.

Midpoint landmarks along the rim of the radioulnar articulation are placed by first anchoring a plane (Plane C) to the points being intersected (Points E and F) and the point along the outermost part of the joint rim between E and F (Point G). In the Figure 6, point E (Landmark 8) is the proximal posterior most point on border of the radioulnar articulation, while

Point F (Landmark 9) is the distal posterior most point. The midpoint between points E and F is point H. A line (Line R) is plotted through points E and F. A line (Line D) is then projected perpendicular to line R on plane C through the midpoint H. The midpoint landmark (Landmark 12) between E and F is placed where Line D intersects the rim of the radioulnar joint. Midpoint landmarks on the radioulnar articulation (Landmarks 11-14) were placed by using the described method (Figure 6).

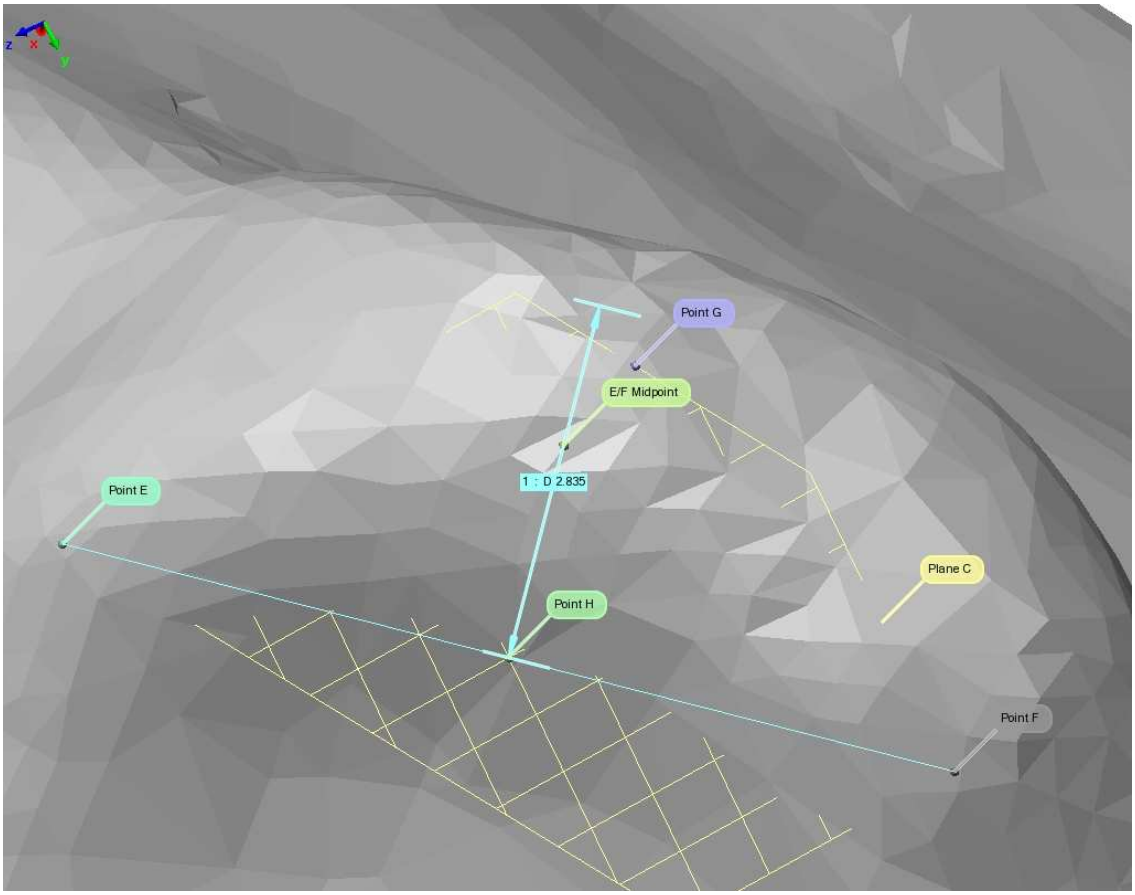

Figure 6.) Male *Homo sapien* (Hosap 496). Points, planes, and lines for placing midpoint landmarks on radioulnar joint. Point E is the proximal posterior most point of the joint and point F is the distal posterior most point of the joint. Line D is shown in teal. Plane C is show in yellow.

The radial midpoint (Landmark 15) was placed by first fitting a plane (plane D) to the radioulnar joint articulation. A line (Line E) is placed perpendicular to the plane through a point located at the midpoint between the landmark at the PA/PP facet and the landmark at the DA/DP

facet. The point of intersection of line E and the model is used as the radial midpoint (point J in Figure 7). It should be noted that the PA facet occupies the same point as posterolateral most point of the humeroulnar articulation.

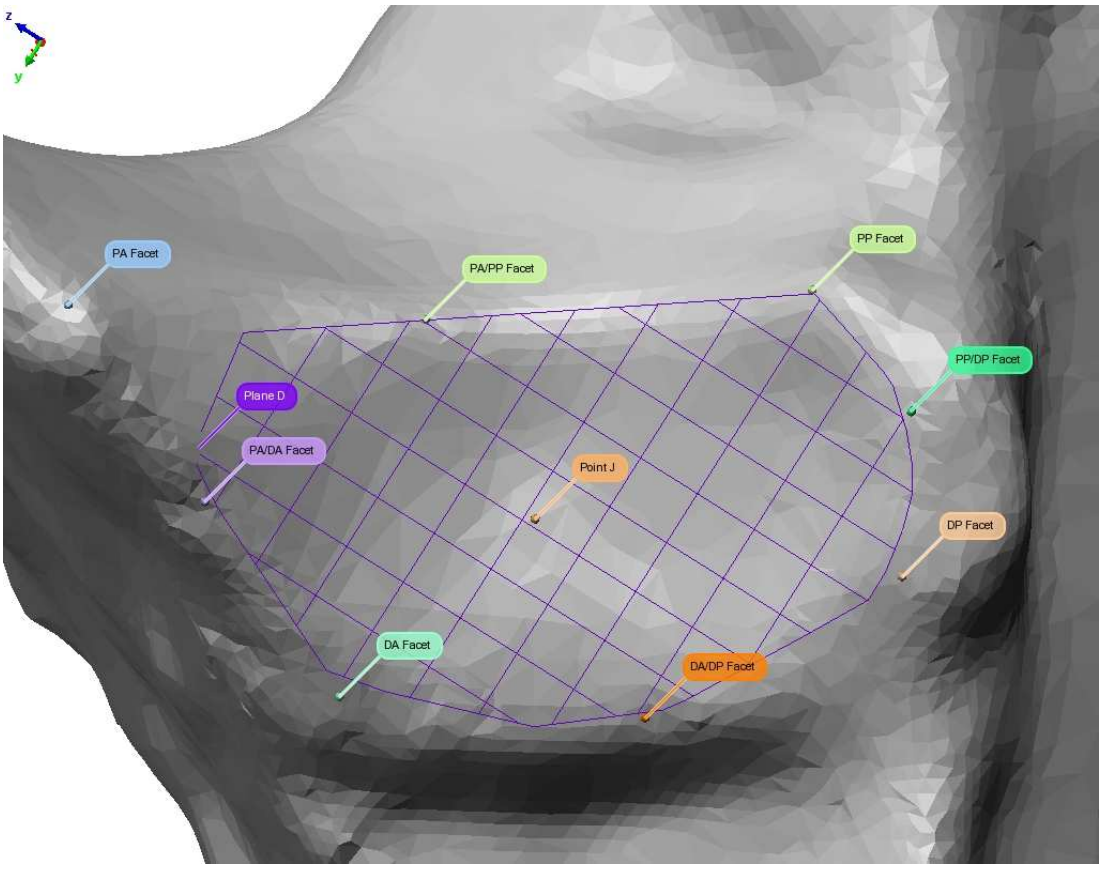

Figure 7.) Male *Homo sapien* (Hosap 496). Points, planes, and lines for placing the Radial Midpoint. Plane D is shown in light purple.

A generalized Procrustes analysis [REF] was used on all models to scale, translate and rotate them to fit with each other as closely as possible. A Principal Component Analysis (PCA) was then applied to the models to see how variance is distributed throughout the species. Both the Procrustes and PCA analysis were accomplished using Morphologika software. The PCA analysis of the data was split into two parts: one PCA to account for size differences between the joints (Procrustes Form Space) and one to negate size differences (solely analyzing shape differences). By removing size based variance, PCA can more accurately pick up on shape

differences between the joints. The first and second principal components were plotted against their respective natural log centroid sizes in order to observe regression lines and possible isometry or allometry in joint shape. A one-way analysis of variance (ANOVA) was used to test the significance of the differences between species and sexes within species along PC1 and PC2 for both PCAs. The F-ratio produced by the ANOVA's shows the degree of difference in the variance of the PC scores. If a comparison of PC scores between sexes in a species yields a high F-ratio, then there may be a significant difference in said sexes along the PC. A Tukey's test was applied post hoc to observe the significance of the differences seen between species and sexes in each ANOVA.

III.) Results

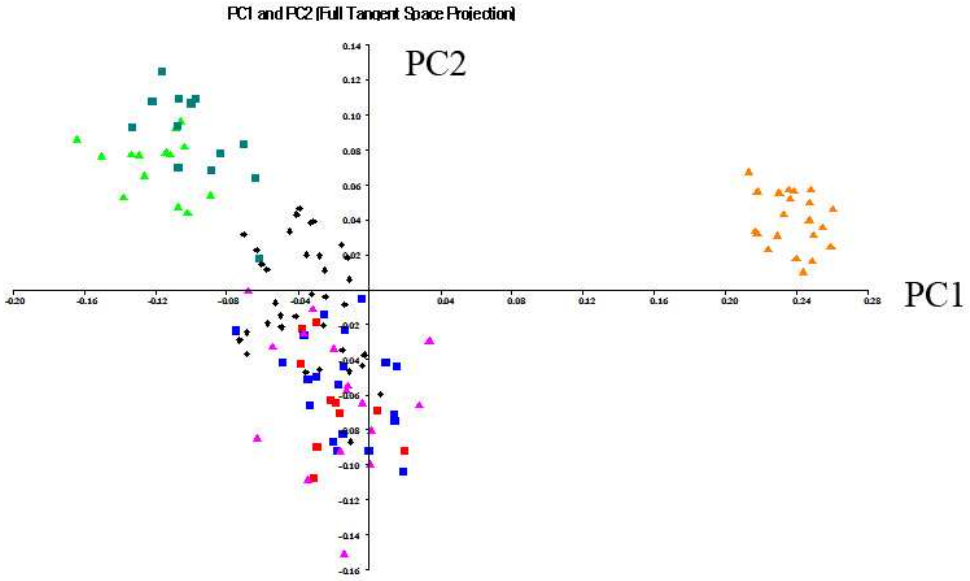

Figure 8.) Shape PC1 and shape PC2 (Full Tangent Space Projection) (Green Triangles=*G. gorilla*, Red Squares= *H. lars*, Black Diamonds=*H. sapiens*, Teal Squares=*P. pygmaeus*, Orange Triangles=*P. cynocephalus*, Purple Triangles=*P. troglodytes* , Blue Squares= *P. troglodytes*). Shape PC1 depicts change in the proportional mediolateral breadth of humeroulnar joint, while shape PC2 depicts change in the proportional anterodistal breadth of the radioulnar joint.

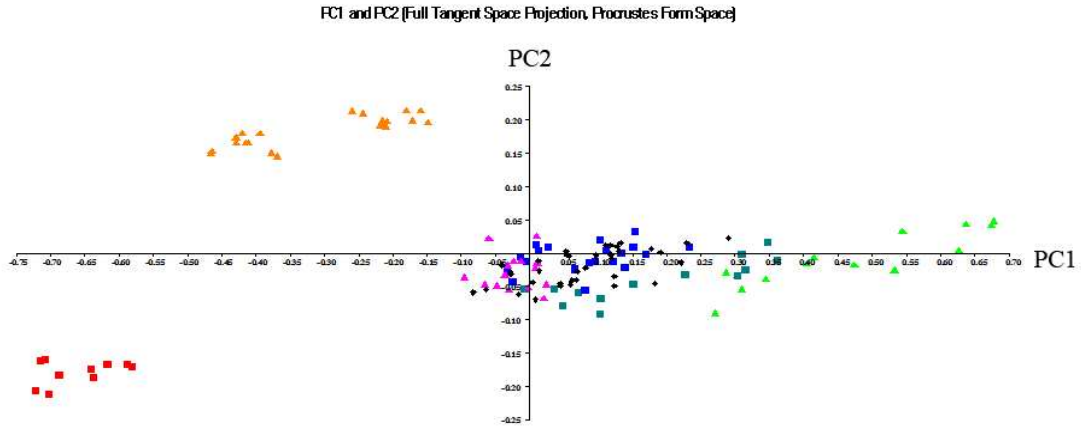

Figure 9.) Size PC1 and size PC2 (Full Tangent Space Projection and Procrustes Form Space) (Green Triangles=*G. gorilla* , Red Squares= *H. lars*, Black Diamonds=*H. sapiens*, Teal Squares=*P. pygmaeus*, Orange Triangles=*P. cynocephalus*, Purple Triangles=*P. troglodytes* , Blue Squares=*P. troglodytes*). Size PC1 depicts change in the raw mediolateral breadth of humeroulnar joint, while size PC2 depicts change in the raw anterodistal breadth of the radioulnar joint.

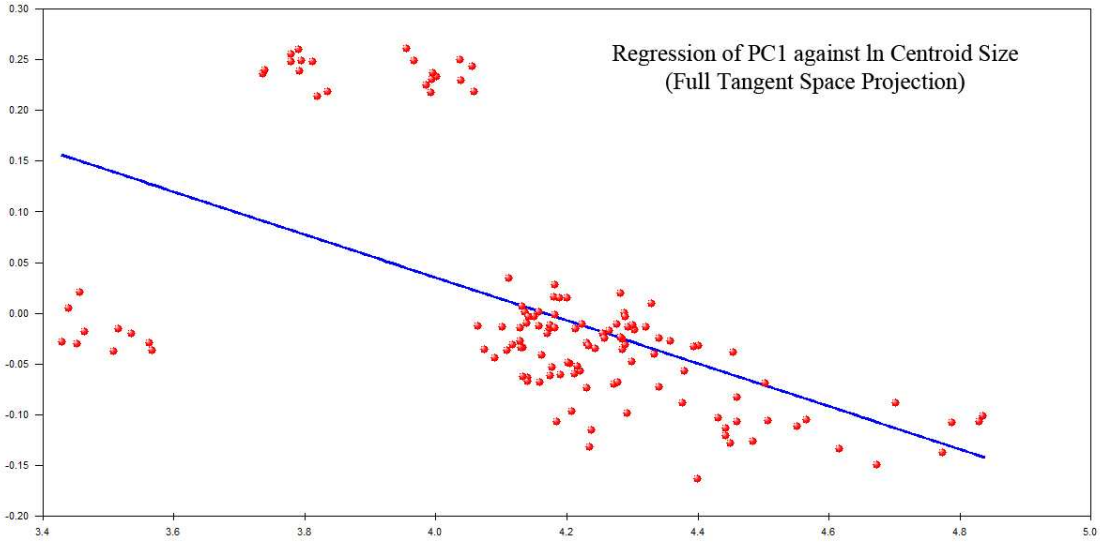

Figure 10.) The regression of shape PC1 against ln Centroid Size (Full Tangent Space Projection) for all species (Ln Centroid Coef=-0.209, Squared Multiple R=0.287, Adjusted squared multiple R=0.281). The line of regression is marked in blue and each ulna specimen is marked in red. The X axis is the natural log centroids sizes and the Y-axis is the PC scores.

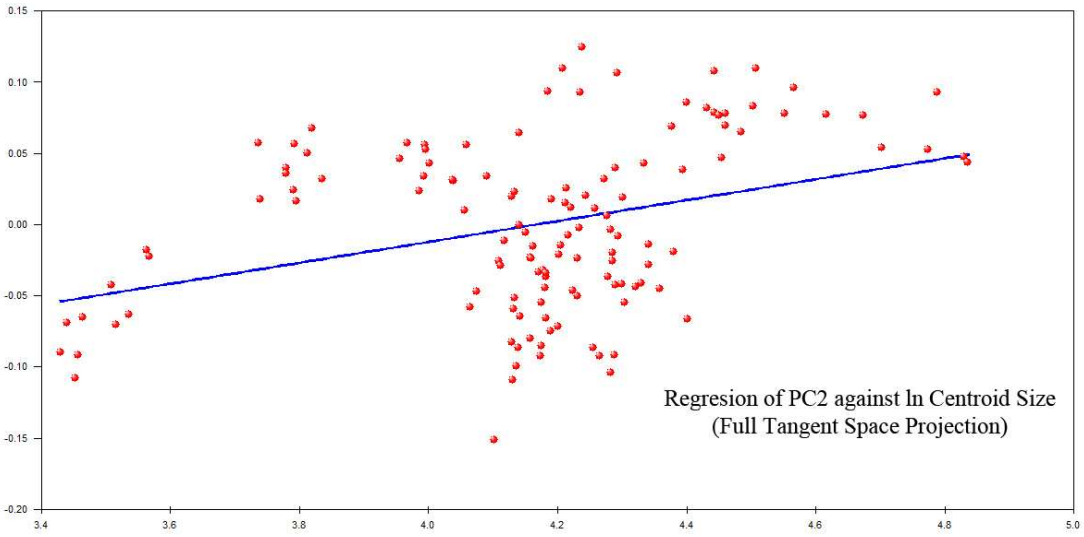

Figure 11.) The regression of shape PC2 against ln Centroid Size (Full Tangent Space Projection) for all species (Ln Centroid Coef=0.071, Squared multiple R=0.114, Adjusted squared multiple R=0.107). The line of regression is marked in blue and each ulna specimen is marked in red. The X axis is the natural log centroids sizes and the Y-axis is the PC scores.

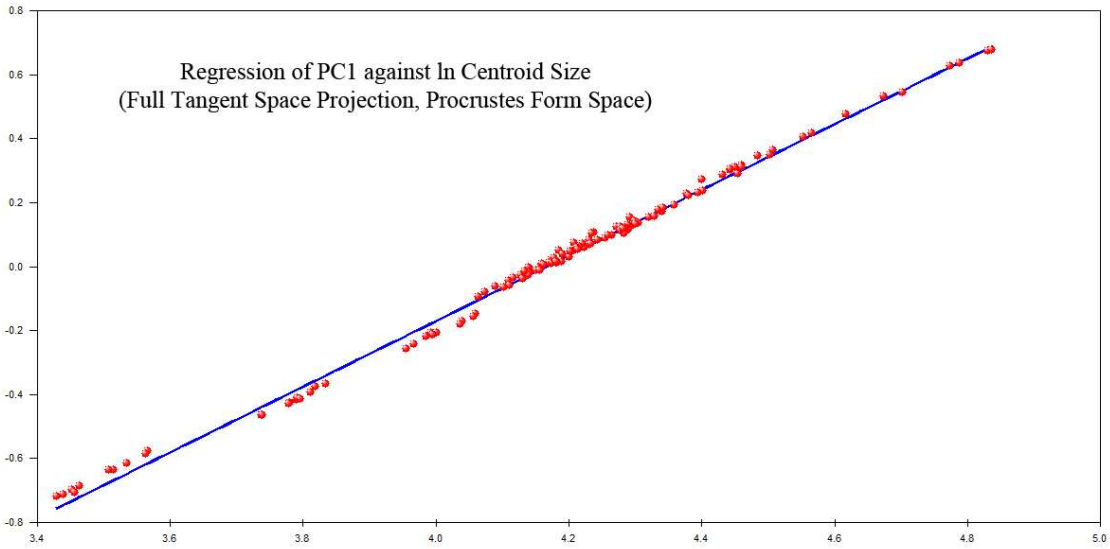

Figure 12.) The regression of size PC1 against ln Centroid Size (Full Tangent Space Projection and Procrustes Form Space) for all species (Ln Centroid Coef=0.936, Squared multiple R=0.826, Adjusted squared multiple=0.825). The line of regression is marked in blue and each ulna specimen is marked in red. The X axis is the natural log centroids sizes and the Y-axis is the PC scores.

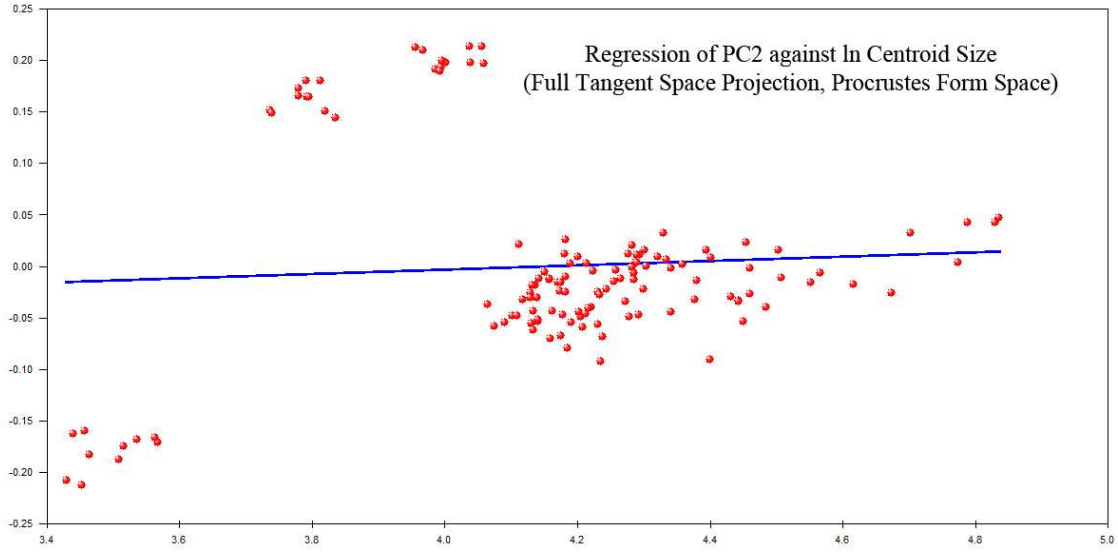

Figure 13.) The regression of size PC2 against ln Centroid Size (Full Tangent Space Projection and Procrustes Form Space) for all species. (Ln Centroid Coef=.005, Squared Multiple R=0.000, Adjusted squared multiple=0.000). The line of regression is marked in blue and each ulna specimen is marked in red. The X axis is the natural log centroids sizes and the Y-axis is the PC scores.

A) Regressions

The regression lines of both shape PC1 (Ln centroid coefficient=-0.209, p=0.000, squared multiple R=0.287) (Figure 10) and shape PC2 (Ln centroid coefficient=0.071, p=0.000, squared multiple R=0.114) (Figure 11) against the natural log centroid size show negative allometry. The regression line of size PC1 against the natural log centroid size shows isometry (Ln centroid coefficient=0.936, p=0.000, squared multiple R=0.826) (Figure 12), showing that the mediolateral breadth of the humeroulnar articulator is consistent as size increases. The regression line of size PC2 against the natural log centroid size shows no correlation (Ln centroid coefficient=0.005, p=0.874, squared multiple R=0.000) (Figure 13). It should be noted that shape PC1, shape PC2, and size PC1 exhibit regression lines that are statistically significant. Size PC2 does not show a regression line that is statistically significant.

Table 2.) Analysis of Variance of shape PC1 and shape PC2 scores (Full Tangent Space Projection) for all species observed (Interspecific variation between sexes). The independent variable in each ANOVA is the species in the sample and the dependent variable is the PC scores. Species exhibit significant difference along both components ($p<0.005$).

	Source	Sum-of-Squares	Df	Mean-Square	F-ratio	P
PC1	Taxa	1.416	1	1.416	856.149	**0.000**
	Error	0.210	127	0.002		
PC2	Taxa	0.039	1	0.039	11.653	**0.001**
	Error	0.429	127			

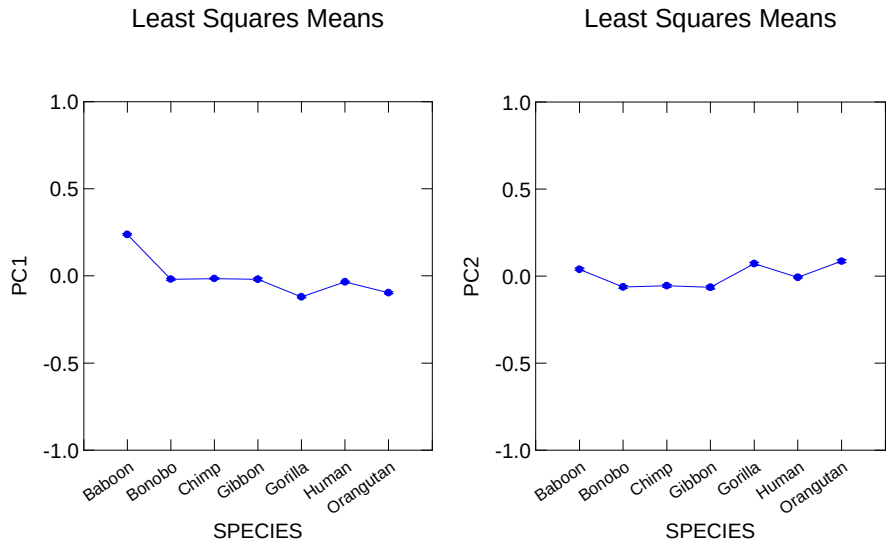

Figure 14.) Least squares means of shape PC1 and shape PC2 scores (Full Tangent Space Projection) for all species observed. The independent variable in each plot is species and the dependent variable is the PC scores.

Table 3.) Matrix of pairwise mean differences for shape PC1 scores (Full Tangent Space Projection) for all species observed.

	P. cyn	P. pan	P. trog	H. lars	G. gor	H. sap	P. pyg
P. cyn	0.000						
P. pan	-0.257	0.000					
P. trog	-0.253	0.004	0.000				
H. lars	-0.257	-0.001	-0.004	0.000			
G. gor	-0.358	-0.101	-0.105	-0.101	0.000		
H. sap	-0.273	-0.016	-0.020	-0.015	0.085	0.000	
P. pyg	-0.334	-0.078	-0.081	-0.077	0.024	-0.062	0.000

Table 4.) Matrix of pairwise mean differences for shape PC2 scores (Full Tangent Space Projection) for all species observed.

	P. cyn	P. pan	P. trog	H. lars	G. gor	H. sap	P. pyg
P. cyn	0.000						
P. pan	-0.102	0.000					
P. trog	-0.094	0.008	0.000				
H. lars	-0.104	-0.002	-0.010	0.000			
G. gor	0.032	0.134	0.126	0.136	0.000		
H. sap	-0.046	0.056	0.048	0.058	-0.078	0.000	
P. pyg	0.047	0.149	0.141	0.151	0.015	0.093	0.000

B.) Interspecific Variation in Shape

In the shape PCA (the PCA without Procrustes Form Space Projection), PC1 and PC2 cumulatively explain 58.77% of the total variance. An Analysis of Variance comparing species via shape PC1 scores ($F=856.149$, $p=0.000$) and shape PC2 scores ($F=11.653$, $p=0.001$) also shows that species vary significantly on both components of the shape PCA (Table 2). Cercopithecoids and Hominoids vary significantly along both shape PC1 and shape PC2. Cercopithecoids exhibit narrow trochlear notches and broad radial notches, whereas Hominoids exhibit relatively broader trochlear notches and narrower radial notches (Figure 14).

A Tukey's post hoc test on shape PC1 shows that *H. sapiens*, *P. troglodytes*, *P. paniscus*, and *H. lars* exhibit significant similarity in means ($p<0.05$) for the proportional mediolateral breadth of the humeroulnar articulator. *G. gorilla* and *P. pygmaeus* also exhibit significant similarities in means while *P. cynocephalus* exhibits no significant similarity to any other species (Table 3).

A Tukey's post hoc test on shape PC2 shows that *P. troglodytes*, *P. paniscus*, *H. lars* exhibits significant similarity in means ($p<0.05$) for the proportional anterodistal breadth of the radioulnar articulator. There also significant similarities in means between *P. cynocephalus*, *H. sapiens*, *G. gorilla*, and *P. pygmaeus* as well as significant similarities between *H. sapiens* and *P. troglodytes* (Table 4).

Table 5.) Analysis of Variance of size PC1 and size PC2 scores (Full Tangent Space Projection and Procrustes Form Space) for all species observed (Interspecific variation between species). The independent variable in each ANOVA is the species in the sample and the dependent variable is the PC scores. Species exhibit significant differences along both components ($p<0.05$).

	Source	Sum-of-Squares	Df	Mean-Square	F-ratio	P
PC1	Taxa	10.116	1	1.686	175.179	**0.000**
	Error	1.174	127	0.010		
PC2	Taxa	1.077	1	0.180	247.366	**0.000**
	Error	0.089	127	0.001		

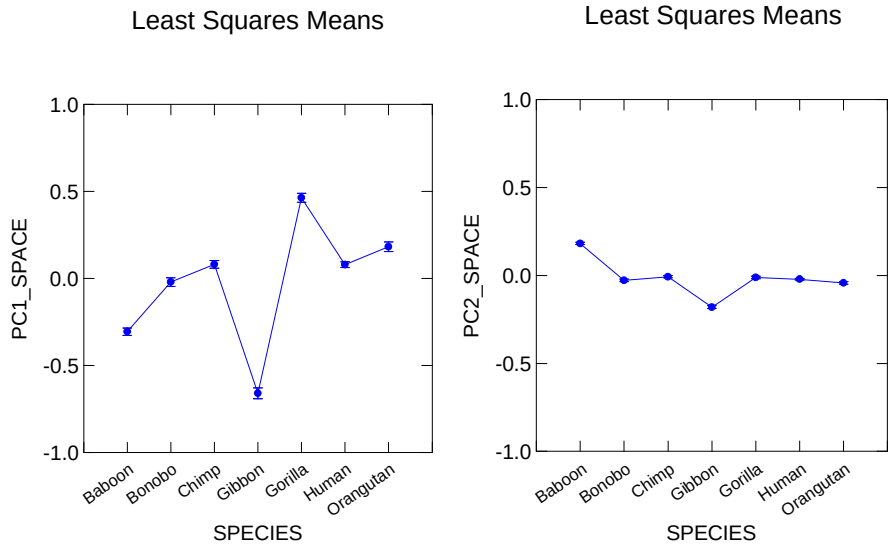

Figure 15.) Least Squares Means of size PC1 and size PC2 scores (Full Tangent Space Projection and Procrustes Form Space) for all species observed, with species as the independent variable and PC scores as the dependent variable.

Table 6.) Matrix of pairwise mean differences for size PC1 scores (Full Tangent Space Projection and Procrustes Form Space) for all species observed.

	P. cyn	P. pan	P. trog	H. lars	G. gor	H. sap	P. pyg
P. cyn	0.000						
P. pan	0.285	0.000					
P. trog	0.387	0.102	0.000				
H. lars	-0.354	-0.639	-0.741	0.000			
G. gor	0.769	0.484	0.382	1.123	0.000		
H. sap	0.385	0.100	-0.001	0.739	-0.384	0.000	
P. pyg	0.488	0.203	0.101	0.842	-0.281	0.103	0.000

Table 7.) Matrix of pairwise mean differences for size PC2 scores (Full Tangent Space Projection and Procrustes Form Space) for all species observed.

	P. cyn	P. pan	P. trog	H. lars	G. gor	H. sap	P. pyg
P. cyn	0.000						
P. pan	-0.210	0.000					
P. trog	-0.190	0.021	0.000				
H. lars	-0.362	-0.152	-0.173	0.000			
G. gor	-0.193	0.017	-0.004	0.169	0.000		
H. sap	-0.204	0.007	-0.014	0.159	-0.010	0.000	
P. pyg	-0.225	-0.015	-0.035	0.137	-0.032	-0.021	0.000

C.) Interspecific Variation in Size

In the size PCA (the PCA with Procrustes Form Space Projection), PC1 and PC2 cumulatively explain 87.6226% of the total variance. An Analysis of Variance comparing species via size PC1 scores ($F=175.179$, $p=0.000$) and size PC2 scores ($F=247.366$, $p=0.000$) shows that species vary significantly from each other on both components of the size PCA (Table 5).

A Tukey's post hoc test on size PC1 shows that *H. sapiens* and *P. troglodytes* exhibit significant similarity in mean ($p<0.05$) for the raw mediolateral breadth of the humeroulnar articulator. With the exception of the similarity observed in *H. sapiens* and *P. troglodytes*, all species exhibit significant mean differences in size PC1 scores (Table 6).

A Tukey's post hoc test on size PC2 shows that there are no significant differences in means ($p<0.05$) for the raw anterodistal breadth of the radioulnar articulator amongst *H. sapiens, P. troglodytes, P. paniscus, G. gorilla,* and *P. pygmaeus*. The size PC2 scores of *P. cynocephalus* and *H. lars*, however, each exhibit significant mean differences ($p>0.05$) from all other primates (Table 7).

Size PC1 shows mediolateral breadth of the humeroulnar joint is greatest in *G. gorilla* and *P. pygmaeus* and smallest in *H.lars* and *P. cynocephalus*. Size PC2 shows that the breadth of the radial notch is greatest in *P. cynocephalus* and least in *H. lars* (Figure 9).

Table 8.) Table of shape ANOVAs (Full Tangent Space Projection) for dimorphism in species along shape PC1 (Intraspecific variation between sexes). Each ANOVA examines the variance in one species, with sex as the independent variable (male or female) and PC scores as the dependent variable. All species exhibit nonsignificant differences in variance (p>0.05).

Species	Sum-of-Squares	Df	Mean-Square	F-ratio	P
P. cynocephalus	0.000	1	0.000	0.635	0.435
P. paniscus	0.000	1	0.000	0.089	0.770
P. troglodytes	0.000	1	0.000	0.005	0.947
H. lars	0.000	1	0.000	0.003	0.959
G. gorilla	0.000	1	0.000	0.109	0.747
H. sapiens	0.000	1	0.000	0.112	0.740
P. pygmaeus	0.000	1	0.000	0.004	0.953

Table 9.) Table of shape ANOVAs (Full Tangent Space Projection) for dimorphism in species along shape PC2 (Intraspecific variation between sexes). Each ANOVA examines the variance in one species, with sex as the independent variable (male or female) and PC scores as the dependent variable. All species exhibit nonsignificant differences in variance (p>0.05).

Species	Sum-of-Squares	Df	Mean-Square	F-ratio	P
P. cyncephalus	0.000	1	0.000	0.001	0.976
P. paniscus	0.005	1	0.005	3.802	0.071
P. troglodytes	0.001	1	0.001	0.653	0.430
H. lars	0.000	1	0.000	0.002	0.966
G. gorilla	0.001	1	0.001	4.604	**0.053**
H. sapiens	0.000	1	0.000	0.257	0.615
P. pygmaeus	0.000	1	0.000	0.003	0.960

Table 10.) Tables of size ANOVAs (Full Tangent Space Projection and Procrustes Form Space) of dimorphism in species along size PC1 (Intraspecific varation between sexes). Each ANOVA examines the variance in one species, with sex as the independent variable (male or female) and PC scores as the dependent variable. *P.cynocephalus*, *P. troglodytes*, *G. gorilla*, and *P. pygmaeus* (bolded) are the only species exhibiting significant differences in variance ($p<0.05$).

Species	Sum-of-Squares	Df	Mean-Square	F-ratio	P
P. cynocephalus	0.241	1	0.241	215.938	**0.000**
P. paniscus	0.002	1	0.002	1.929	0.187
P. troglodytes	0.031	1	0.031	7.466	**0.014**
H. lars	0.000	1	0.000	0.043	0.842
G. gorilla	0.240	1	0.240	50.910	**0.000**
H. sapiens	0.000	1	0.000	0.635	0.435
P. pygmaeus	0.184	1	0.184	73.635	**0.000**

Table 11.) Tables of size ANOVAs (Full Tangent Space Projection and Procrustes Form Space) of dimorphism in species along size PC2 (Intraspecific variation between sexes). Each ANOVA examines the variance in one species, with sex as the independent variable (male or female) and the PC scores as the dependent variable. *P. cynocephalus*, *G. gorilla*, and *P. pygmaeus* (bolded) are the only species exhibiting significant differences in variance ($p<0.05$).

Species	Sum-of-Squares	Df	Mean-Square	F-ratio	P
P. cynocephalus	0.008	1	0.008	64.301	**0.000**
P. paniscus	0.000	1	0.000	0.223	0.644
P. troglodytes	0.001	1	0.001	1.631	0.218
H. lars	0.000	1	0.000	0.058	0.816
G. gorilla	0.011	1	0.011	13.012	**0.004**
H. sapiens	0.000	1	0.000	0.001	0.976
P. pygmaeus	0.184	1	0.184	73.635	**0.000**

D.) Sexual Shape Dimorphism

Sexes do not vary significantly in shape for any species along shape PC1 and shape PC2 ($p>0.05$) (Table 8, Table 9).

E.) Sexual Size Dimorphism

Size PC1 shows that there are significant differences in size between sexes amongst *G. gorilla*, *P. troglodytes*, *P. pygmaeus*, and *P. cynocephalus* ($p<0.05$) (Table 10). Size PC2 shows that *G. gorilla*, *P. pygmaeus*, and *P. cynocephalus* exhibit significant differences in variance between the sexes ($p<0.05$), while *P. troglodytes* shows no significant difference between sexes ($p>0.05$) (Table 11).

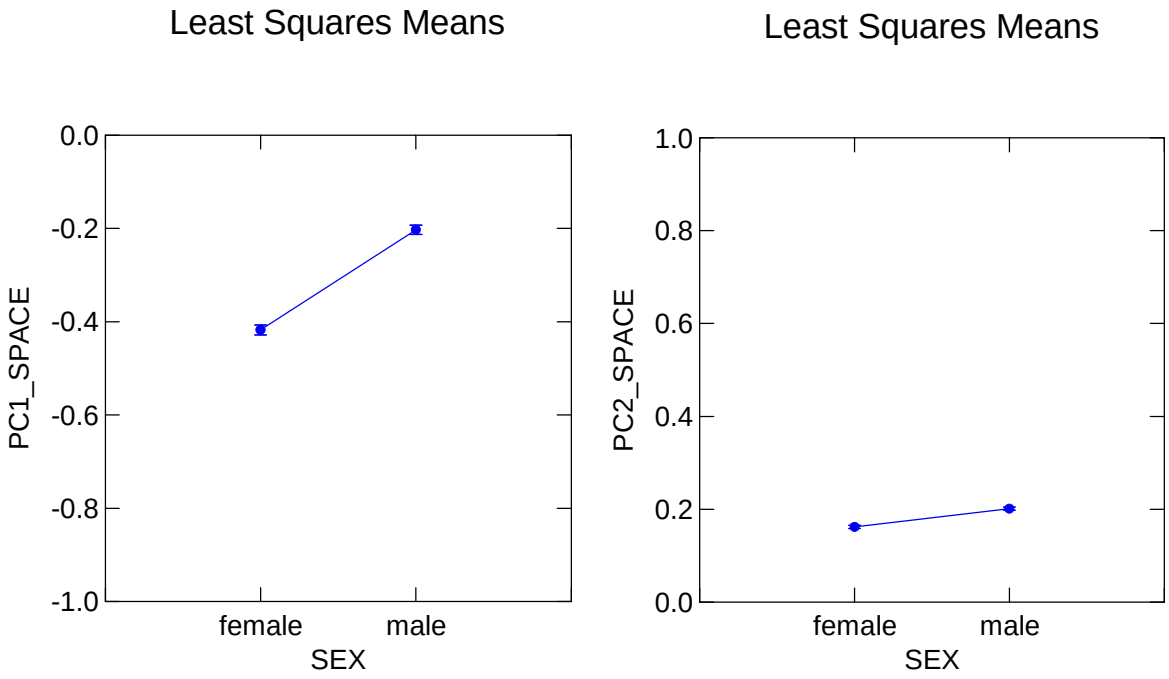

Figure 16.) Plot Least Squares Means for size ANOVA (Full Tangent Space Projection and Procrustes Form Space) of dimorphism in *P. cynocephalus* along size PC1 and size PC2. The independent variable for each plot is sex (male or female). The dependent variable is PC scores.

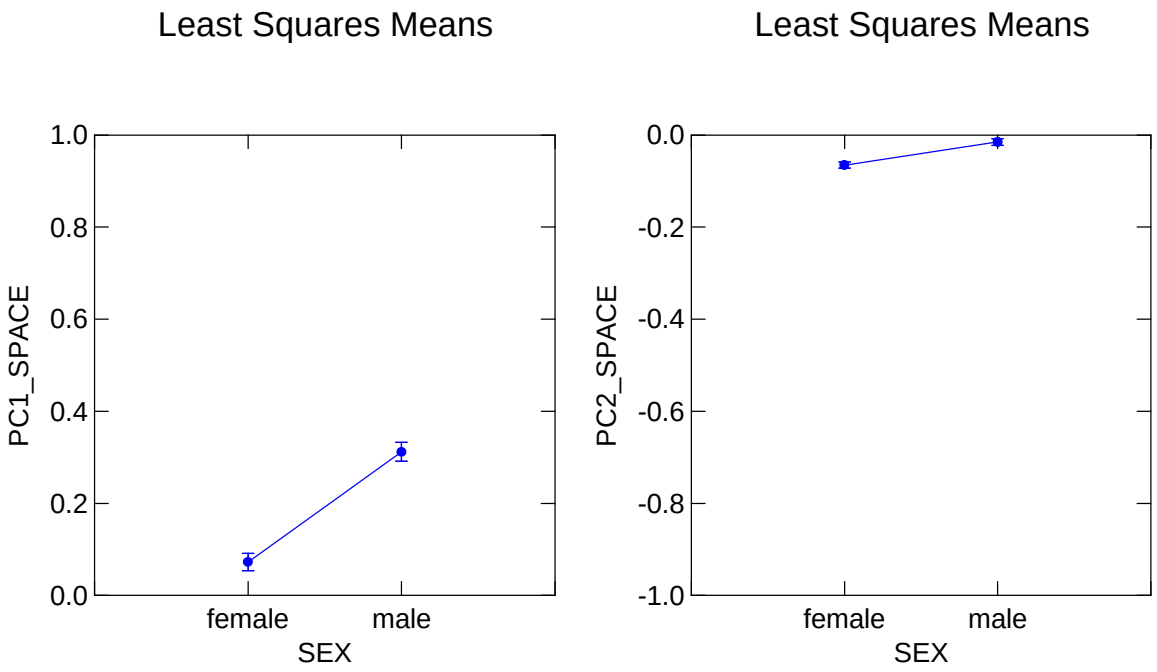

Figure 17.) Least Squares Means for size ANOVA (Full Tangent Space Projection and Procrustes Form Space) of Dimorphism in *P. pygmaeus* along size PC1 and size PC2. The independent variable for each plot is sex (male or female). The dependent variable is PC scores.

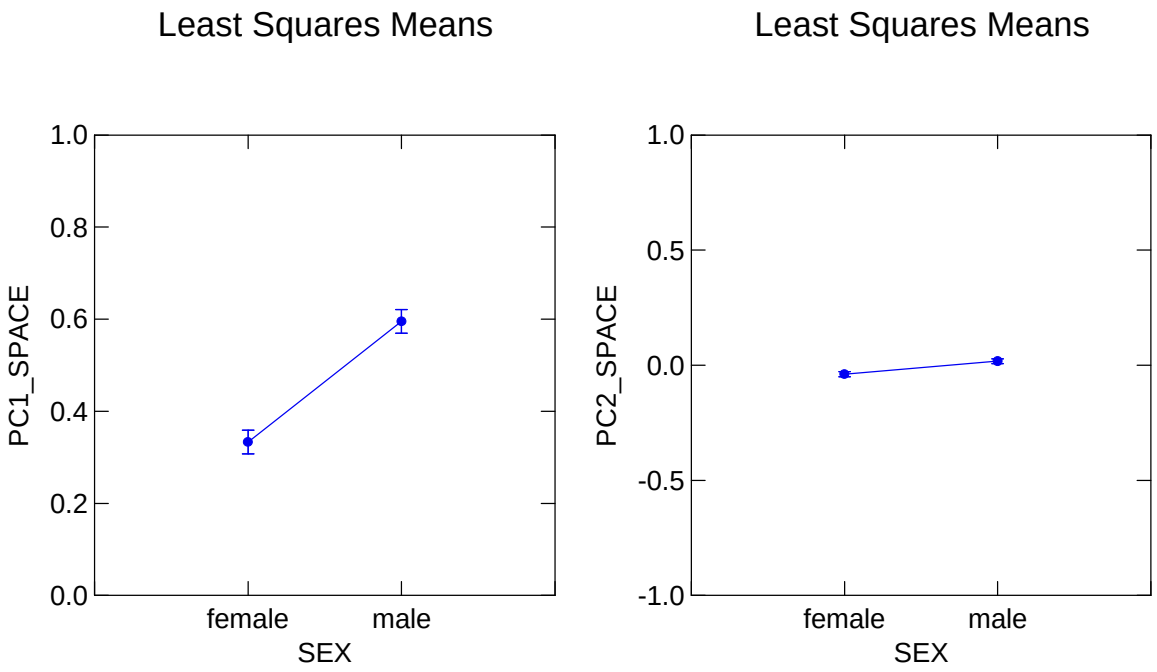

Figure 18.) Least Squares Means for size ANOVA (Full Tangent Space Projection and Procrustes Form Space) of Dimorphism in *G. gorilla* along size PC1 and size PC2. The independent variable for each plot is sex (male or female). The dependent variable is PC scores.

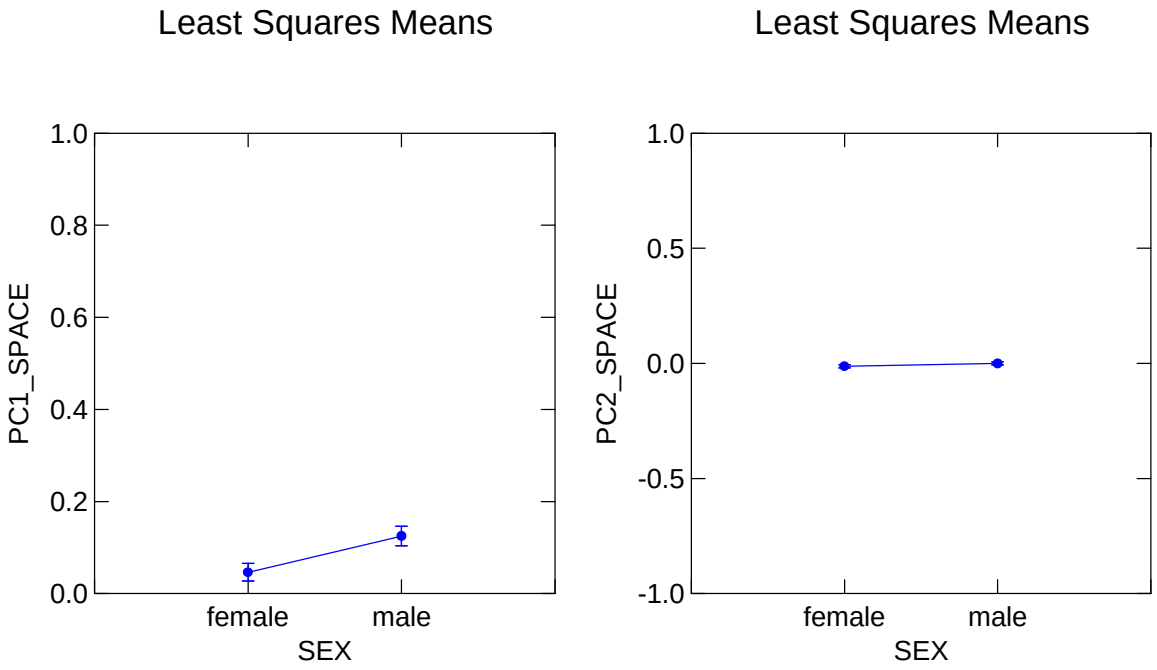

Figure 19.) Plot of Least Squares Means for size ANOVA (Full Tangent Space Projection and Procruste Form Space) of dimorphism in *P. troglodytes* along size PC1 and size PC2. The independent variable for each plot is sex (male or female). The dependent variable is PC scores.

IV.) Discussion

The findings from the analysis support the hypothesis that the magnitude of sexual dimorphism correlates with differences in joint size. Large bodied primates all exhibit larger joints with larger body size, but no significant shape change is observed between sexes of the same species. As such, one can reject that hypothesis that significant interspecific variance in joint shape exists between males and females of the same species.

The sexes of *G. gorilla* show a difference in intraspecific variance along shape PC2 that is close to significant (p=0.053): this probability may be a byproduct of the relatively small sample size of *G. gorilla* (7 male, 7 female). Though some primate species may exhibit differences in habitual behavior between sexes, said differences are not so great as to cause functional differences in joint morphology. There was no consistent sample for the analysis and the sample size for sexes in all species were relatively small (n<30). Though the mediolateral breadth of the elbow joint appears to scale isometrically with size, larger samples and a consistent sample size would be needed to confirm any of the observed results. Bootstrapping can provide greater consistency if not enough bones can be collected to even out each species sample.

The regression of size PC1 against the natural log centroid size shows that the mediolateral breadth of the humeroulnar joint scales isometrically with body size (Ln centroid coefficient=0.936, p=0.000, Squared multiple R=0.826) (Figure 12). No other regression showed a clear correlation between PC scores and the natural log centroid size.

The F-ratios effectively show the magnitude of difference between males and females in each species. One can observe that for size PC1 the F-ratio is greatest in *P. cynocephalus*, the species most distantly related to *H. sapiens*. The smaller the F-ratio the closer a species is

related to *H. sapiens*, the exception being *P. paniscus*, in which case the low sexual size dimorphism can be inferred to be an independently derived trait. The sexes in *P. troglodytes* show sexual size dimorphism in the mediolateral breadth of the proximal ulna articulator, whereas *P. paniscus* shows none (Table 10). *P. troglodytes* are highly aggressive and territorial relative to *P. paniscus* and the sexual dimorphism exhibited by the former is a byproduct of this aggressive behavior (Doran 1993 (1), Fleagle 2013). Male and female *H. lars*, a species that is known to exhibit little sexual dimorphism, do not exhibit a significant difference in variance in the breadth of both the humeroulnar and radioulnar articulator. The *H. sapiens* sample also exhibits no sexual size dimorphism, which corresponds with the overall trend of lessening sexual dimorphism in the genus *Homo*. The observed magnitudes of size dimorphism in the mediolateral breadth of the humeroulnar match similar findings of dimorphism in body mass and canine morphology (Leigh and Shea 1995, Plavcan 2001, Plavcan 2011).

The findings from the analysis support the hypothesis that the magnitude of sexual dimorphism correlates with difference in joint size. Figure 12 shows how the size PC1 scales isometrically with the natural log centroid size of each specimen, a variable that reflects the overall size of the ulna. Large bodied primates all exhibit larger joints with larger body size, but little change in joint shape. It can be inferred that differences in locomotor behavior due to bodyweight are not so extreme as to cause proportional shape differences in the proximal ulna, at least as observed from the chosen landmarks.

The regressions of PC1 and PC2 of the shape PCA are significant, however the squared multiple R for both regressions show a low goodness-of-fit (Figure 10, Figure 11). It may be that the differences in shape observed between cercopithecoids and hominoids are obstructing the analysis. The regression of size PC2 shows the lowest goodness-of-fit, and it can likewise be

inferred that P. cynocephalus is obstructing the analysis (Figure 13). Size PC1 is the only principal component that reliably shows scaling (Figure 12). The regression observed in Figure 12 shows that the raw mediolateral breadth of the humeroulnar articulator scales with body size in all species. The regressions of shape PC1, shape PC2 and size PC2 do not show any correlation with body size. Observing Figures 8, 9, 10, and 13, it is apparent that *P. cynocephalus*, the species showing the most obvious body size dimorphism, is obfuscating the regression of the other species. It may be that sexual dimorphism and articulator adaptations have diverged in *P. cynocephalus* to the point where they are an outlier to the other species in the analysis. In the future an analysis of sexual dimorphism of solely cercopithecoids may illuminate how sexual dimorphism in cercopithecoids differs from hominoids. *P. cynocephalus* is an out-group in an analysis that has placed greater emphasis on hominoids; such an analysis cannot hope to accurately examine sexual dimorphism amongst all catarrhines.

Joint morphology does appear to distinguish primate taxa. The raw mediolateral breadth of the humeroulnar articulator is greatest in *G. gorilla* and *P. pygmaeus*, the primates in the analysis that exhibit the greatest bodyweight. Shape PC1 shows change in the proportional mediolateral breadth of the humeroulnar articulator, showing how the joint becomes broader or narrower in shape in a given species (Figure 8). For both *G. gorilla* and *P. pygmaeus*, the proportional mediolateral breadth of the humeroulnar joint is greatest among males and can be inferred to be a means of supporting the larger bodyweights exhibited by males in each species.

H. sapiens and *P. troglodytes* exhibit similar measurements in the mediolateral breadth of the humeroulnar articulator (Table 6). *P. troglodytes* are the most recent ancestor of *H. sapiens* out of all the species observed; the similarities in size observed in the humeroulnar joint may be

an ancestral condition to both species, however there is currently no fossil evidence supporting this conjecture.

The raw mediolateral breadth of the humeroulnar articulator is narrowest in *H. lars*. *H. lars* is a primarily suspensory primate and the narrowness observed in the humerounlar articulator may be attributed to how *H. lars* subjects its elbow joint almost exclusively to tension during locomotion. In comparison *G. gorilla* and *P. pygmaeus* subject their bones to extreme compression due their greater bodyweight and utilization of terrestrial locomotion.

The raw anterodistal breadth of the radioulnar articulator appears to be similar amongst all hominoids with the exception of *H. lars*. *P. cynocephalus* also exhibit dissimilarity to all other primates observed (Table 7). *H. lars* exhibits the anterodistally narrowest radioulnar articulators out of all the species examined. In comparison *P. cynocephalus* exhibits the anterodistally broadest radioulnar articulators. *P. cynocephalus* is exclusively terrestrial in its locomotion and exhibit anteriorly oriented radioulnar articulators to stabilize their forearms during locomotion. The broadness of the radioulnar articulator exhibited by *P. cynocephalus* may be an adaptation to increase the service area of the joint for stabilizing the joint. *P. troglodytes*, *P. paniscus*, *G. gorilla*, and *P. pygmaeus* exhibit similar anterodistal breadths in their radioulnar articulators, which may be attributed to their utilization of both arboreal and terrestrial locomotion. The anterodistal breadth of the radioulnar articulator exhibited by *H. sapiens* can be inferred to be an ancestral trait plesiomorphic for all hominoids observed with the exception of *H. lars*.

It does not appear, however, that any specific locomotor behavior correlates with a specific joint shape. A Tukey's post hoc test of the shape PC1 scores shows that *G. gorilla* and *P. pygmaeus* are grouped, but there are significant differences in the locomotor behavior of each

species. Joint shape does appear to change with bodyweight, however the bodyweight differences between sexes is not shown to be significant enough to produce shape differences within any observed species. Given the results of the analyses one can be assured that the taxonomic classification of the proximal ulna in fossil catarrhines is not being distorted by shape dimorphism. If a collection of proximal ulna fossils (all known to be catarrhines) exhibits similar morphology but differ in size, one can hypothesize that there may be sexual dimorphism in said fossils. The isometry observed in the regression of size PC1 against the natural log centroid size is consistent with limb scaling patterns observed across catarrhine primates. As such, one can hypothesize that fossil catarrhines may exhibit similar scaling patterns with the pattern observed in extant species being an ancestral trait (Steudel 1982, Swartz 1989, Godfrey 1991).

An analysis of just the proximal ulna is insufficient to fully understand how sexual dimorphism affects morphology and scaling in the elbow joint. Past studies have typically analyzed either one or two bones in the elbow joint. Patel found that the radial head in monkeys is ovoid with an eccentrically positioned fovea whereas in hominoids it is more circular with a distinct bevel on the medial aspect between the proximal and distal articular surfaces. One can differentiate between terrestrial quadrupedalism and arboreal suspension based on the different morphologies observed in the proximal radius (Patel 2005 (2)). In the distal humerus, the elbow joint is size dimorphic relative to the given degree (overall magnitude of difference) of body size dimorphism. Lague found that mountain gorillas exhibit dimorphism in the distal humerus that ranges from similar to far below the expected for similarity between sexes. It is suspected that, amongst African apes, large bodied males experience considerably greater joint stresses than females; the large mobile joints may diminish stress to the point that positive allometry is not

needed (Lague 2000). However, all the bones in the elbow are utilized in locomotor and positional behavior. The elbow joint can be better understood if it is analyzed as an integrated unit rather than as individual parts. Differences in morphology may become apparent when all three articulations are analyzed cumulatively rather than separately. In the future I propose an analysis of all three bones of the elbow via their articulations sites. Such an analysis would require an extensive sample of bones taken from multiple collections, but 3-D modeling via polyworks should make the procuring of said bones relatively simple. I hypothesize that such an analysis, should it be undertaken, would yield an overall more precise and accurate investigation of dimorphism in the elbow joint.

In conclusion, the sexes in certain species show significant variance in the raw mediolateral breadth of the humeroulnar articulator and the raw anterodistal breadth of the radioulnar articulator, however there are no corresponding significant differences in the proportions of said articulators. Significant differences in joint size between males and females were found to correlate with the magnitude of sexual dimorphism. Significant interspecific variance in joint shape was not found to exist between males and females of the same species; differences in locomotor behavior between sexes do not appear to be strong enough to facilitate differences in morphology. A more systematic study with a larger sample size will be needed to verify the observed results. Special thanks to Dr. Plavcan, Dr. Ungar, and Dr. Nolan for agreeing to be part of my thesis committee and Dr. Plavcan in particular for providing the 3-D models and statistical programs used in the analysis.

V.) References

Abdala, Virginia and Rui Diego. Comparative Anatomy, Homologies and Evolution of the Pectoral and Forelimb Musculature of Tetrapods with Attention to Extant Amphibians and Reptiles. Journal of Anatomy. Vol. 217. 2010. 536-573.

Cant, John G.H. Effects of Sexual Dimorphism in Body Size on Feeding Postural Behavior of Sumatran Orangutans (*Pongo pygmaeus*). American Journal of Physical Anthropology. Vol 74. 1987. 143-148.

Diego, Rui and Bernard Wood. Soft-Tissue Anatomy of the Primates: Phylogenetic Analyses Based on the Muscles of the Head, Neck, Pectoral Region and Upper Limb, with notes on the Evolution of the Muscles. Journal of Anatomy. Vol. 219. 2011. 273-359.

Diego, Rui, Brian G. Richmond, and Bernard Wood. Evolution and Homologies of Primate and Modern Human Hand and Forearm Muscles, with Notes on Thumb Movements and Tool Use. Journal of Human Evolution. Vol. 63. 2012. 64-78.

Doran, Diane M. Comparative Locomotor Behavior of Chimpanzees and Bonobos: The Influence of Morphology on Locomotion. American Journal of Physical Anthropology. Vol.91. 1993. 99-115.

Doran, Diane M. Sex Differences in Adult Chimpanzee Positional Behavior: Thee Influence of Body Size on Locomotion and Posture. American Journal of Physical Anthropology. Vol. 91. 1993. 83-98.

Drapeau, Michelle S.M. Articular Morphology of the Proximal Ulna in Extant and Fossil Hominoids and Hominins. Journal of Human Evolution. Vol. 55. 2008. 86-102.

Fairbairn, Daphne .J. Allometry for Sexual Size Dimorphism: Pattern and Process in the Coevolution of Bodysize in Males and Females. Annual Review of Ecology and Systematics. Vol. 28. 1997. 659-687.

Feldesman, M.R. The Primate Forelimb. 1976.

Feldesman, M.R. Morphometric Analysis of the Distal Humerus of some Cenozoic Catarrhines: The Late Divergence Hypothesis Revisited. Physical Anthropology. 1982. 73-95.

Fleagle, John G. Primate Adaptation and Evolution, 3rd Edition. 2013.

Godfrey, Laurie. Scaling of Limb Joint Surface Areas in Anthr0poid Primates and Other Mammals. Journal of Zoology. Vol. 223. 1991. 603-625.

Gould, Stephen Jay. Allometry and Size in Ontogeny and Phylogeny. Biological Reviews of the Cambridge Philosophical Society. Vol. 41. 1966.

Jenkins, F.A. The Functional Anatomy and Evolution of the Mammalian Humeroulnar Articulation . American Journal of Anatomy. Vol. 137. 1973. 281-298.

Lague, Michael R. and William L. Jungers. Patterns of Sexual Dimorphism in the Hominoid Distal Humerus. Journal of Human Evolution. Vol. 36. 1999. 379-399.

Lague, Michael R. Patterns of Sexual Dimorphism in the Joint Surfaces of the Elbow and Knee of Catarrhine Primates. 2000.

Lague, Michael R. Patterns of Joint Size Dimorphism in the Eblow and Knee of Catarrhine Primates. American Journal of Physical Anthropology. Vol. 120. 2003. 278-297.

Leigh, Steven R. and Brian T. Shea. Ontogeny and the Evolution of Adult Body Size Dimorphism in Apes. American Journal of Primatology. Vol. 36. 1995. 37-60.

Patel, B.A. Form and Function of the Oblique Cord (*chorda oblique*) in Anthropoid Primates. Primates. Vol. 46. 2005. 47-57.

Patel, B.A. The Hominoid Proximal Radius: Re-Interpreting Locomotor Behavior in Early Hominins. Journal of Human Evolution. Vol. 48. 2005. 415-432.

Plavcan, Michael J. and Carel P. Van Schaik. Intrasexual Competition and Body Weight Dimorphism in Anthropoid Primates. American Journal of Physical Anthropology. Vol. 103. 1997. 37-68.

Plavcan, Michael J. Sexual Dimorphism in Primates. Yearbook of Physical Anthropology. Vol. 44. 2001. 25-53.

Plavcan, Michael J. Understanding dimorphism as a Function of Changes in Male and Female Traits. Evolutionary Anthropology. Vol 20. 2011. 143-155.

Regan, William D., Sarah L. Korinek, Bernard F. Morrey, and Kai-Nan An. Biomechanical Study of Ligaments Around the Eblow Joint. Clinical Orthopaedics and Related Research. Vol. 271. 1991. 170-179.

Richmond, Brian G., John G. Fleagle, John Kappelman, and Carl C. Swisher III. First Hominoid from the Miocene of Ethiopia and the Evolution of the Catarrhine Elbow. American Journal of Physical Anthropology. Vol 105. 1998. 257-277.

Rockwell, Laura Christie. The Evolutionary Biology of the Hominoid Elbow Joint: Inter and Intra-specific Allometry of the Articular Surfaces. 1994.

Rose, M.D. Another Look at the Anthropoid Elbow. Journal of Human Evolution. Vol. 17. 1988. 193-224.

Ruff, C.B. and Runestad. Primate Limb Bones Structural Adaptations. Annual Review of Anthropology. Vol. 21. 1992. 407-433.

Schmitt, Daniel. Mediolateral Reaction Forces and Forelimb Anatomy in Quadrupedal Primates: Implications for Interpreting Locomotor Behavior in Fossil Primates. Journal of Human Evolution. Vol. 44. 2003. 47-58.

Steudel, Karen. Allometry and Adaptation in the Catarrhine Postcranial Skeleton. American Journal of Physical Anthropology. Vol. 59. 1982. 431-441.

Swartz, Sharon M. The Functional Morphology of Weight-Bearing: Limb Joint Surface Area Allometry in Anthropoid Primates. Journal of Zoology. Vol. 218. 1989. 441-460.

White, Tim D., Michael T. Black, and Pieter A Folkens. Human Osteology 3rd Edition. 2012.